11th World Congress on Computational Mechanics (WCCM XI)
5th European Conference on Computational Mechanics (ECCM V)
6th European Conference on Computational Fluid Dynamics (ECFD VI)
E. Oñate, J. Oliver and A. Huerta (Eds)

AN SGBEM FORMULATION FOR COHESIVE DELAMINATION MODEL WITH COULOMB FRICTION

JOZEF KŠIŇAN*, ROMAN VODIČKA†

Technical University of Košice, Civil Engineering Faculty
Department of Structural Mechanics*, Department of Applied Mathematics†
Vysokoškolská 4, 042 00 Košice, Slovakia
e-mail: jozef.ksinan@tuke.sk*, roman.vodicka@tuke.sk†, web page: http://www.svf.tuke.sk

Key words: Interface Damage, Symmetric Galerkin Boundary Element Method, Cohesive Contact, Frictional Contact, Quadratic Programming.

Abstract. Recently, the advance in analysis and development of composite laminate structures has considerably influenced the applicability of composite materials in aeronautical and aircraft industry. Therefore, considering the mathematical models and developing of numerical algorithms for investigation of the interface fracture problems in such structures seems to be crucial. The interface as a contact boundary zone of a layered structure has been modeled as an infinitesimally thin cohesive layer which can be partially or completely damaged. The numerical implementation considers the cohesive-type contact which includes nonlinear phenomenon of friction and also elasto-viscosity. A mathematical model for analysis of delamination problems has been developed and implemented into the program MATLAB by means of the Symmetric Galerkin Boundary Element Method. The approach enables to exploit an energetic formulation, which governs the process of interface rupture.

1 INTRODUCTION

Numerical solution of contact problems with friction may be very challenging. There exist several approaches for the solution of contact problems by Boundary Element Method (BEM), see e.g. [5] and references therein. The present work tries to enhance the energetic model of interface debonding proposed in [6] in order to cover also the frictional contact between the debonded parts of a specimen or structure. In the present work, the frictional law is regularized to cope with the energetic character of the model, see [4]. The regularization is proposed so that convex quadratic energy functionals are obtained and algorithms of quadratic programming can successfully be applied. This includes, first, replacing of the standard Signorini contact conditions by normal compliance contact condition replacement, which allows a small overlapping of solids in contact, and, second, making the bulk domains visco-elastic, although the parameters characterizing the viscous response of the structure are small. In the following sections

the proposed model is described, its numerical solution is outlined and an example is solved to assess the applicability of the approach to contact problems.

2 CONTACT MODEL

For the sake of simplicity, only two-dimensional contact problems between two solids, Ω^η ($\eta = A,B$), will be considered in the present work. The standard *Signorini condition of unilateral contact* $t_n[\mathbf{u}]_n = 0$, $t_n \leq 0$, $[\mathbf{u}]_n \geq 0$ in the contact zone Γ_c is replaced by the normal compliance penalization condition $t_n = k_g[\mathbf{u}]_n^-$, $[\mathbf{u}]_n^-$ denotes the negative part of the relative normal displacement. This penalization can also be explained by presence of a very thin layer of the normal stiffness $k_g \gg 0$ which is compressed in contact and stress-free out of contact. Here, the relative normal displacement $[\mathbf{u}]_n = (\mathbf{u}^B - \mathbf{u}^A)\cdot\mathbf{n}^A$ is defined at the contact zone. Similarly, the relative tangential displacement $[\mathbf{u}]_s$ can be also defined, as shown in Figure 1. Also, $\mathbf{t}$ denotes the traction vector and t_n its normal component.

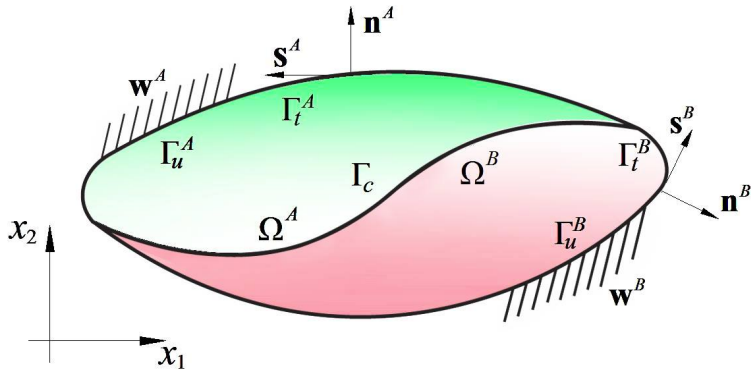

Figure 1: A model – contact of two subdomains.

The solution of the contact problem is based on the evolution of energies during the loading process: the elastic energy stored in the bulks and the energy dissipated due to friction and (possibly a very small amount) due to viscosity. From a physical point of view, frictional dissipation in our model is given by the functional $\mathscr{R}(\mathbf{u};\dot{\mathbf{u}}) = \int_{\Gamma_c} -\mu k_g [\mathbf{u}]_n^- \cdot [\dot{\mathbf{u}}]_s \mathrm{d}\Gamma$ where the rate of change of the relative tangential displacement as a function of time $[\mathbf{u}]_t$ is denoted by $[\dot{\mathbf{u}}]_t$. The model also includes the classical *Coulomb friction law* $|t_s| \leq \mu |t_n|$ with a constant friction coefficient $\mu \geq 0$ as a relation between normal and tangential tractions, t_n and t_s. The viscosity is considered by a simple linear *Kelvin-Voigt* model which provides the stress tensor σ by the relation $\sigma = \mathbf{C}:\varepsilon(\mathbf{u}) + \mathbf{D}:\varepsilon(\dot{\mathbf{u}})$ where $\mathbf{D}$ expresses the fourth-order tensor of viscosity parameters, given in the present work as $\mathbf{D} = \tau_R \mathbf{C}$, where $\tau_R \geq 0$ is a relaxation time parameter.

2.1 Cohesive-type contact interface model

Actual trends at engineering practise usually consider an approach which supposes the nonlinear continuous material response of the mechanical stress σ and damage parameter ζ. This

approach thus refers to a *cohesive-type model*. The cohesive formulation assumes that the displacement discontinuities $\delta_i\,(i=1,2,3)$ across the crack are related to the *traction vector t*, in a zone located ahead of the crack tip, usually called *cohesive zone*. An effective approach to achieve the continuous non-linear material response is by means of the energy approach formulation of *stored energy functional* $\mathscr{E}$, see [3].

The failure mechanism starts, when the mechanical stress σ, linearly increasing with u until the *driving force* σ_d is achieved, reaches activations threshold *fracture energy* G_d . Consequently ζ starts to evolve from one non-linearly until it arrives to zero, see Figure 2. This can

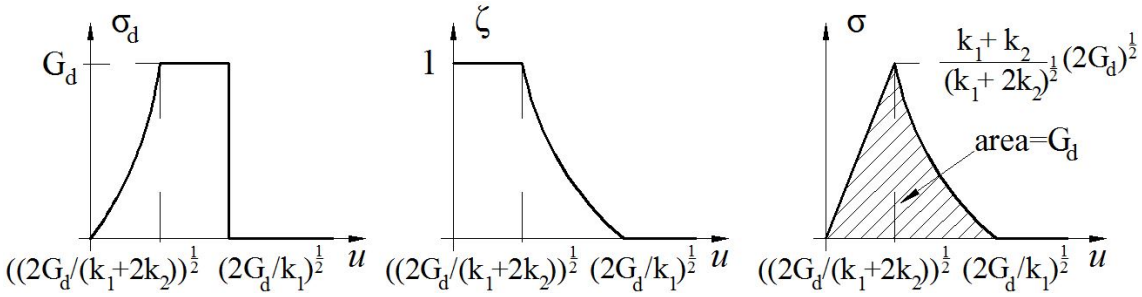

Figure 2: Cohesive contact response of the driving force σ_d, the damage ζ and the mechanical stress σ.

be obtained by adding a new delamination quadratic term ζ^2 and a stiffness parameter k_2 so that the mechanical stress decays as

$$\sigma = \left(k_1\zeta + k_1\zeta^2\right)u. \tag{1}$$

The main feature of cohesive proposed model is that energy functional is separately quadratic both in the $\mathbf{u}$ and ζ variable. Therefore it enables to apply *quadratic programming algorithms* for solving *minimization problem*, see [1], [4]. Based on the above assumptions, a quasi-static visco-elastic evolution is governed by the following inclusions:

$$\begin{aligned} \partial_{\mathbf{u}}\mathscr{E}(\tau,\mathbf{u},\zeta) + \mathscr{R}_{\dot{\mathbf{u}}}(\mathbf{u};\dot{\mathbf{u}},\dot{\zeta}) + \delta_{\mathbf{u}}\mathscr{F}(\tau,\mathbf{u}) \ni 0,\\ \partial_{\zeta}\mathscr{E}(\tau,\mathbf{u},\zeta) + \mathscr{R}_{\dot{\zeta}}(\mathbf{u};\dot{\mathbf{u}},\dot{\zeta}) \ni 0, \end{aligned} \tag{2}$$

where the symbol ∂ refers to partial subdifferential relying on the convexity of the energy functionals, see [2], [3]. It includes the stored energy functional [3], in a form:

$$\begin{aligned} \mathscr{E}(\tau,\mathbf{u},\zeta) = \int_{\Omega^A}\frac{1}{2}\boldsymbol{\varepsilon}^A{:}\mathbf{C}^A{:}\boldsymbol{\varepsilon}^A\mathrm{d}\Omega + \int_{\Omega^B}\frac{1}{2}\boldsymbol{\varepsilon}^B{:}\mathbf{C}^B{:}\boldsymbol{\varepsilon}^B\mathrm{d}\Omega + \\ \int_{\Gamma_c}\frac{1}{2}[\zeta(k_{n_1}+\zeta k_{n_2})[\mathbf{u}]_n^2 + \zeta(k_{s_1}+\zeta k_{s_2})[\mathbf{u}]_s^2 + k_g([\mathbf{u}]_n^-)^2]\mathrm{d}\Gamma, \end{aligned} \tag{3}$$

with the admissible displacements $\mathbf{u}^\eta = \mathbf{w}^\eta(\tau)$ on Γ_u^η and the small strain tensor $\boldsymbol{\varepsilon}^\eta = \boldsymbol{\varepsilon}(\mathbf{u}^\eta)$, the potential energy of external forces (acting only along the boundary in the present work):

$$\mathscr{F}(\tau,\mathbf{u}) = -\int_{\Gamma_t^A}\mathbf{f}^A\cdot\mathbf{u}^A\mathrm{d}\Gamma - \int_{\Gamma_t^B}\mathbf{f}^B\cdot\mathbf{u}^B\mathrm{d}\Gamma, \tag{4}$$

and the dissipation potential

$$\mathscr{R}(\mathbf{u};\dot{\mathbf{u}},\dot{\zeta}) = \int_{\Gamma_c} -\mu k_g [\mathbf{u}]_n^- \cdot |[\dot{\mathbf{u}}]_s| + G_d|\dot{\zeta}| + \alpha|\dot{\zeta}|^2 \mathrm{d}\Gamma + \tau_R \int_{\Omega^A} \frac{1}{2}\dot{\varepsilon}^A{:}\mathbf{C}^A{:}\dot{\varepsilon}^A \mathrm{d}\Omega + \tau_R \int_{\Omega^B} \frac{1}{2}\dot{\varepsilon}^B{:}\mathbf{C}^B{:}\dot{\varepsilon}^B \mathrm{d}\Omega, \quad (5)$$

where $\dot{\varepsilon}^\eta = \varepsilon(\dot{\mathbf{u}}^\eta)$ is the strain rate.

3 COMPUTER IMPLEMENTATION

The numerical procedure devised for solving the above problem considers time and spatial discretization separately, as usual. The procedure is formulated in terms of the boundary data only, with the spatial discretization leading to the Symmetric Galerkin BEM (SGBEM) [5], [6].

3.1 TIME DISCRETIZATION

The time-stepping scheme is defined by a fixed time step size τ_0 such that $\tau^k = k\tau_0$ for $k=1,\dots\frac{T}{\delta}$. The displacement rate is approximated by the finite difference $\dot{\mathbf{u}} \approx \frac{\mathbf{u}^k - \mathbf{u}^{k-1}}{\tau_0}$, where $\mathbf{u}^k$ denotes the solution at the discrete time τ^k. Similarly the damage parameter can be defined $\dot{\zeta} \approx \frac{\zeta^k - \zeta^{k-1}}{\tau_0}$. The differentiation with respect to the displacement rate can be replaced by the differentiation with respect to $\mathbf{u}$ and ζ as well, i.e. $\partial_{\dot{\mathbf{u}}}\mathscr{R}(\mathbf{u};\dot{\mathbf{u}},\dot{\zeta}) \approx \tau_0 \partial_{\mathbf{u}}\mathscr{R}(\mathbf{u}^{k-1}; \frac{\mathbf{u}-\mathbf{u}^{k-1}}{\tau_0}, \frac{\zeta-\zeta^{k-1}}{\tau_0})$ and $\partial_{\dot{\zeta}}\mathscr{R}(\mathbf{u};\dot{\mathbf{u}},\dot{\zeta}) \approx \tau_0 \partial_{\zeta}\mathscr{R}(\mathbf{u}^{k-1}; \frac{\mathbf{u}-\mathbf{u}^{k-1}}{\tau_0}, \frac{\zeta-\zeta^{k-1}}{\tau_0})$. It means that the inclusion is approximated at discrete times τ^k by the first order optimality condition for the functional

$$\mathscr{H}^k(\mathbf{u},\zeta) = \mathscr{E}(k\tau_0,\mathbf{u},\zeta) + \tau_0 \mathscr{R}(\mathbf{u}^{k-1}; \frac{\mathbf{u}-\mathbf{u}^{k-1}}{\tau_0}, \frac{\zeta-\zeta^{k-1}}{\tau_0}) + \mathscr{F}(k\tau,\mathbf{u}). \quad (6)$$

The optimality solution is denoted by $\mathbf{u}^k$. Substituting the previous time-step result into the dissipation potential due to friction makes the pertinent functional convex with respect to the unknown $\mathbf{u}$, the optimality solution being thus unique and defining the minimum. The simple viscosity model is chosen in order to exploit the reformulation of the visco-elastic problem in the bulk in terms of an elastic problem in the bulk, which is solved by the elastostatic SGBEM [2]. Let us introduce a new variable $\mathbf{v}$ (a fictitious displacement), which will replace the admissible $\mathbf{u}$ for the time step k, as

$$\mathbf{v} = \mathbf{u} + \tau_R \frac{\mathbf{u}-\mathbf{u}^{k-1}}{\tau_0}, \quad \text{and also} \quad \mathbf{v}^k = \mathbf{u}^k + \tau_R \frac{\mathbf{u}^k - \mathbf{u}^{k-1}}{\tau_0}. \quad (7)$$

Then, the functional $\mathscr{H}^k$ is defined as

$$\mathscr{H}^k(\mathbf{v},\zeta)=\frac{\tau_0}{\tau_0+\tau_R}\left[\frac{1}{2}\int_{\Omega^A}\varepsilon(\mathbf{v}^A):\mathrm{C}^A:\varepsilon(\mathbf{v}^A)\mathrm{d}\Omega+\frac{1}{2}\int_{\Omega^B}\varepsilon(\mathbf{v}^B):\mathrm{C}^B:\varepsilon(\mathbf{v}^B)\mathrm{d}\Omega+\right.$$
$$\left.\frac{1}{2}\frac{\tau_0}{\tau_0+\tau_R}\int_{\Gamma_c}\zeta(k_{n_1}+\zeta k_{n_2})[\mathbf{u}]_n^2+\zeta(k_{s_1}+\zeta k_{s_2})[\mathbf{u}]_s^2+k_g([\mathbf{v}+\frac{\tau_R}{\tau_0}\mathbf{u}^{k-1}]_n^-)^2\mathrm{d}\Gamma\right]$$
$$+\int_{\Gamma_c}-\frac{\tau_0\mu k_g}{\tau_0+\tau_R}[\mathbf{u}^{k-1}]_n^-\cdot|[\mathbf{v}-\mathbf{u}^{k-1}]_s|-G_d\left(\zeta-\zeta^{k-1}\right)+\frac{\alpha}{2\tau_0}\left(\zeta-\zeta^{k-1}\right)^2\mathrm{d}\Gamma$$
$$+\frac{1}{2}\frac{\tau_R}{\tau_0}\int_{\Omega^A}\varepsilon(\mathbf{u}^{Ak-1}):\mathrm{C}^A:\varepsilon(\mathbf{u}^{Ak-1})\mathrm{d}\Omega+\frac{1}{2}\frac{\tau_R}{\tau_0}\int_{\Omega^B}\varepsilon(\mathbf{u}^{Bk-1}):\mathrm{C}^B:\varepsilon(\mathbf{u}^{Bk-1})\mathbf{d}\Omega$$
$$-\int_{\Gamma_t^A}\mathbf{f}^A\cdot\ (\mathbf{v}^A+\frac{\tau_R}{\tau_0}\mathbf{u}^{Ak-1})\mathrm{d}\Gamma-\int_{\Gamma_t^B}\mathbf{f}^B\cdot\ (\mathbf{v}^B+\frac{\tau_R}{\tau_0}\mathbf{u}^{Bk-1})\mathrm{d}\Gamma,\quad(8)$$

or any admissible $\mathbf{v}$ satisfying the condition

$$\mathbf{v}^\eta=\mathbf{w}^\eta(k\tau)+\frac{\tau_R}{\tau_0}\big(\mathbf{w}^\eta(k\tau)-\mathbf{w}^\eta((k-1)\tau)\big)=\tilde{\mathbf{w}}^\eta(k\tau)\text{ on }\Gamma_u^\eta\text{ and}0\le\zeta\le\zeta^{k-1}\text{on}\Gamma_c.\quad(9)$$

Let $\mathbf{v}^k$=argmin$\mathscr{H}^k(\mathbf{v})$. It is worth observing that the viscosity in (8) is eliminated in the sense that the only energy term in the bulk associated to the unknown $\mathbf{v}$ is the elastic strain energy, $\mathbf{u}^{k-1}$ is known from the previous time step. In finding the minimum of $\mathscr{H}^k(\mathbf{v})$, an iteration for $\mathbf{v}$ is rendered as a solution of an elastic BVP for unknown (fictitious) displacements $\mathbf{v}$ and the actual tractions $\mathbf{t}$ of the visco-elastic model. For the solution of these BVPs an SGBEM code is used, thus using in the minimization process only such solutions, it is convenient to change the bulk integrals with $\mathbf{v}$ in to boundary based integrals

$$\int_{\Omega^\eta}\varepsilon(\mathbf{v}^\eta):C^\eta:\varepsilon(\mathbf{v}^\eta)\mathbf{d}\Omega=\int_{\Gamma^\eta}\mathbf{t}^\eta(\mathbf{v}^\eta)\cdot\mathbf{v}^\eta\mathrm{d}\Gamma.\quad(10)$$

Once $\mathbf{v}^k$ is obtained it can be transformed back to the original solution $\mathbf{u}^k$ by the relation.

3.2 Spatial discretization and SGBEM

The role of the SGBEM in the present computational procedure is to provide a complete boundary-value solution from the given boundary data for each domain in order to calculate the elastic strain energy in these domains by using the boundary integral in(10). Thus, the SGBEM code calculates unknown tractions along $\Gamma_c\cup\Gamma_u$, assuming the displacements at Γ_c to be known from the used minimization procedure, in the same way as proposed and tested in [4], [5], [6]. The integral equations solved by SGBEM are the Somigliana displacement and traction identities, written for each particular domain Ω^η separately. The numerical solution is obtained by the piecewise linear approximations of the form

$$\mathbf{v}^\eta(x)=\sum_p\mathbf{N}^\eta_{\psi p}(x)\mathbf{v}^\eta_p,\quad\mathbf{t}^\eta(x)=\sum_l\mathbf{N}^\eta_{\varphi l}(x)\mathbf{t}^\eta_l,\quad(11)$$

with nodal shape functions $\mathbf{N}^{\eta}_{\psi p}(x)$ and $\mathbf{N}^{\eta}_{\varphi l}(x)$ and nodal values $\mathbf{v}^{\eta}_{p}$ and $\mathbf{t}^{\eta}_{l}$. Let the subvectors of the nodal unknowns at the boundary parts Γ_u^{η}, Γ_t^{η} and Γ_c, respectively, be distinguished by the same subscripts u, t and c. Then, SGBEM leads to the symmetric square matrix of the following system of linear algebraic equations:

$$\begin{pmatrix} -\mathbf{U}^{\eta}_{uu} & \mathbf{T}^{\eta}_{ut} & -\mathbf{U}^{\eta}_{uc} \\ \mathbf{T}^{\eta T}_{tu} & -\mathbf{S}^{\eta}_{tt} & \mathbf{T}^{\eta T}_{tc} \\ -\mathbf{U}^{\eta}_{cu} & \mathbf{T}^{\eta}_{ct} & -\mathbf{U}^{\eta}_{cc} \end{pmatrix} \begin{pmatrix} \mathbf{t}^{\eta}_{u} \\ \mathbf{v}^{\eta}_{t} \\ \mathbf{t}^{\eta}_{c} \end{pmatrix} = \begin{pmatrix} -\frac{1}{2}\mathbf{M}^{\eta}_{uu} - \mathbf{T}^{\eta}_{uu} & \mathbf{U}^{\eta}_{ut} & -\mathbf{T}^{\eta}_{uc} \\ \mathbf{S}^{\eta}_{uu} & \frac{1}{2}\mathbf{M}^{\eta T}_{tt} - \mathbf{T}^{\eta T}_{tt} & \mathbf{S}^{\eta}_{tc} \\ -\mathbf{T}^{\eta}_{cu} & \mathbf{U}^{\eta}_{ct} & -\frac{1}{2}\mathbf{M}^{\eta}_{cc} - \mathbf{T}^{\eta}_{cc} \end{pmatrix} \begin{pmatrix} \mathbf{g}^{\eta} \\ \mathbf{f}^{\eta} \\ \mathbf{v}^{\eta}_{c} \end{pmatrix}. \quad (12)$$

The elements of the submatrices denoted with letters **U**, **T** and **S** are formed by double integrals including the singular integral kernels denoted by the same letter as is usual in SGBEM, see [6]. The square 2×2 submatrices, associated with the nodes l and p, of the mass matrices $\mathbf{M}^{\eta}_{rr}$ (with r=$u,t,$ or c), are formed by the integrals:

$$(\mathbf{M}^{\eta}_{rr})_{lp} = \int_{\Gamma_r^{\eta}} \mathbf{N}^{\eta}_{\varphi l}(x)\mathbf{N}^{\eta}_{\psi p}(x)\mathrm{d}\Gamma. \quad (13)$$

3.3 MINIMIZATION ALGORITHM

Once all the boundary data (displacements and tractions) are obtained from the solution of , the energy of the state given by $\mathscr{H}^k$ in (8) can be calculated using (10). It is worth to see how it is carried out in the present implementation. First, let us reconsider the absolute value term and the term with $[\cdot]^-$ in $\mathscr{H}^k$. A classical trick of removing the unpleasant terms and replacing them by additional unknowns with restrictions is used [6]. Let the additional auxiliary unknowns be denoted as α and β and the following restrictions hold:

$$\begin{aligned} \alpha - [\mathbf{v}]_s &\geq -\left[\mathbf{u}^{k-1}\right]_s, & \beta &\geq 0, \\ \alpha + [\mathbf{v}]_s &\geq \left[\mathbf{u}^{k-1}\right]_s, & \beta + [\mathbf{v}]_n &\geq -\frac{\tau_R}{\tau_0}\left[\mathbf{u}^{k-1}\right]_n. \end{aligned} \quad (14)$$

For the discretization, the approximation formulas for both auxiliary parameters α, β given by pertinent boundary element mesh should be considered. In what follows, the same mesh and approximation as used in (11) for displacements on the boundary part Γ_c^A is considered. The approximation formulas can be written in the form:

$$\alpha(x) = \sum_m N_{\psi m}(x)\alpha_m, \quad \beta(x) = \sum_m N_{\psi m}(x)\beta_m, \quad \zeta(x) = \sum_m N_{\zeta m}(x)\zeta_m, \quad (15)$$

where α_m, β_m are the nodal unknowns pertinent to the node x_m^A.

Then, the discretized energy $\mathscr{H}^k$, from equation (8) using (10) and approximations (11) and (15) is expressed as

$$\begin{aligned}
&\frac{\tau_0+\tau_R}{\tau_0}\mathscr{H}^k(\mathbf{v},\alpha,\beta,\zeta) = \\
&\qquad \int_{\Gamma^A}\frac{1}{2}\sum_p \mathbf{N}^A_{\psi p}(x)\mathbf{v}^A_p \cdot \sum_l \mathbf{N}^A_{\varphi l}(x)\mathbf{t}^A_l \mathrm{d}\Gamma + \int_{\Gamma^B}\frac{1}{2}\sum_q \mathbf{N}^B_{\psi q}(x)\mathbf{v}^B_q \cdot \sum_r \mathbf{N}^B_{\varphi r}(x)\mathbf{t}^B_r \mathrm{d}\Gamma \\
&+\int_{\Gamma_c}\left[\frac{1}{2}\left(\left(\sum_m N_{\zeta m}(x)\zeta_m\right)k_{n1}+\left(\sum_n N_{\zeta n}(x)\zeta_n\right)^2 k_{n2}\right)\left(\sum_q N^B_{\psi sq}(x)u^B_{sq}-\sum_p N^A_{\psi sp}(x)u^A_{sp}\right)^2\right. \\
&\quad +\frac{1}{2}\left(\left(\sum_m N_{\zeta m}(x)\zeta_m\right)k_{s1}+\left(\sum_n N_{\zeta n}(x)\zeta_n\right)^2 k_{s2}\right)\left(\sum_q N^B_{\psi sq}(x)u^B_{sq}-\sum_p N^A_{\psi sp}(x)u^A_{sp}\right)^2 \\
&\qquad \left.+\mu k_g\left(\sum_q N^{AB}_{npq}u^{Bk-1}_{nq}-u^{Ak-1}_{np}\right)^-\left(\sum_q N_{\psi q}(x)\alpha_q\right)\right]\mathrm{d}\Gamma \\
&\qquad +\int_{\Gamma_c} -G_d\left(\sum_n N_{\zeta n}(x)(\zeta_n-\zeta_n^{k-1})\right)+\frac{\alpha}{2\,\tau_0}(\sum_n N_{\zeta n}(x)(\zeta_n-\zeta_n^{k-1}))^2\mathrm{d}\Gamma \\
&\qquad -\int_{\Gamma^A_t}\sum_p \mathbf{N}^A_{\psi p}(x)\mathbf{v}^A_p\cdot\sum_l \mathbf{N}^A_{\varphi l}(x)\mathbf{f}^A_l\mathrm{d}\Gamma-\int_{\Gamma^B_t}\sum_q \mathbf{N}^B_{\psi q}(x)\mathbf{v}^B_q\cdot\sum_r \mathbf{N}^B_{\varphi r}(x)\mathbf{f}^B_r\mathrm{d}\Gamma \\
&\qquad +\mathscr{V}(\mathbf{u}^{Ak-1},\mathbf{u}^{Bk-1},\mathbf{f}^{Ak},\mathbf{f}^{Bk}), \quad (16)
\end{aligned}$$

where $N^{AB}_{pq}{=}N^B_{\psi q}(x^A_p)$. The functional $\mathscr{V}$ includes all the data which are constant with respect to $\mathbf{v}$. In minimization of the functional (16) with the restrictions (14), it may be useful to reformulate the problem in such a way that the restrictions change to bound constraints. The left-column and right-column restrictions in (14) provide linearly independent constraints which can respectively be written in a matrix form as

$$\begin{pmatrix}\mathbf{I}^A & -\mathbf{N}^{AB}_s & \mathbf{I}^A\\ \mathbf{I}^A & \mathbf{N}^{AB}_s & -\mathbf{I}^A\end{pmatrix}\begin{pmatrix}\alpha\\ \mathbf{v}^B_s\\ \mathbf{v}^A_s\end{pmatrix}\geq\begin{pmatrix}\xi_1\\ \xi_2\end{pmatrix},\qquad \begin{pmatrix}\mathbf{I}^A & \mathbf{0} & \mathbf{0}\\ \mathbf{I}^A & \mathbf{N}^{AB}_n & -\mathbf{I}^A\end{pmatrix}\begin{pmatrix}\beta\\ \mathbf{v}^B_n\\ \mathbf{v}^A_n\end{pmatrix}\geq\begin{pmatrix}\mathbf{0}\\ \xi_3\end{pmatrix}, \quad (17)$$

with the identity matrix $\mathbf{I}^A$, the matrices $\mathbf{N}^{AB}_n$ and $\mathbf{N}^{AB}_s$ consisting of N^{AB}_{pq} and ξ_i corresponding to the right-hand sides in (14). Both inequalities are defined by full row-rank matrices. Thus, denoting arbitrary matrices whose columns span respectively the null-spaces of the left-hand-side matrices in (17) by $\mathbf{K}_\alpha$ and $\mathbf{K}_\beta$, the following relations hold:

$$\begin{pmatrix}\alpha\\ \mathbf{v}^B_s\\ \mathbf{v}^A_s\end{pmatrix}=\begin{pmatrix}\mathbf{I}^A & \mathbf{I}^A\\ -\left(\mathbf{N}^{AB}_s\right)^T & \left(\mathbf{N}^{AB}_s\right)^T\\ \mathbf{I}^A & -\mathbf{I}^A\end{pmatrix}\begin{pmatrix}\mathbf{N}^{AB}_s\left(\mathbf{N}^{AB}_s\right)^T+2\mathbf{I}^A & -\mathbf{N}^{AB}_s\left(\mathbf{N}^{AB}_s\right)^T\\ -\mathbf{N}^{AB}_s\left(\mathbf{N}^{AB}_s\right)^T & \mathbf{N}^{AB}_s\left(\mathbf{N}^{AB}_s\right)^T+2\mathbf{I}^A\end{pmatrix}^{-1}\begin{pmatrix}\mathbf{y}_1\\ \mathbf{y}_2\end{pmatrix}+\begin{pmatrix}\mathbf{K}^\alpha_\alpha\\ \mathbf{K}^B_\alpha\\ \mathbf{K}^A_\alpha\end{pmatrix}\mathbf{z}_\alpha, \quad (18a)$$

with the restrictions applied only to $\mathbf{y}_i$: $\begin{pmatrix}\mathbf{y}_1\\ \mathbf{y}_2\end{pmatrix} \geq \begin{pmatrix}\xi_1\\ \xi_2\end{pmatrix}$ and

$$\begin{pmatrix}\beta\\ \mathbf{v}_s^B\\ \mathbf{v}_s^A\end{pmatrix} = \begin{pmatrix}\mathbf{I}^A & \mathbf{I}^A\\ \mathbf{0} & \left(\mathbf{N}_n^{AB}\right)^T\\ 0 & -\mathbf{I}^A\end{pmatrix} \begin{pmatrix}\mathbf{I}^A & \mathbf{I}^A\\ \mathbf{I}^A & \mathbf{N}_n^{AB}\left(\mathbf{N}_n^{AB}\right)^T + 2\mathbf{I}^A\end{pmatrix}^{-1} \begin{pmatrix}\mathbf{y}_3\\ \mathbf{y}_4\end{pmatrix} + \begin{pmatrix}\mathbf{K}_\beta^\beta\\ \mathbf{K}_\beta^B\\ \mathbf{K}_\beta^A\end{pmatrix} \mathbf{z}_\beta,$$

$$\text{with } \begin{pmatrix}\mathbf{y}_3\\ \mathbf{y}_4\end{pmatrix} \geq \begin{pmatrix}0\\ \xi_3\end{pmatrix}. \quad (18b)$$

Thus, there is the same number of bound constraints as provided by the more general restrictions (14). The discretized functional (16) can be expressed in a general matrix form as

$$\mathscr{H}^k(\mathbf{y}) = \frac{1}{2}\mathbf{y}^T\mathbf{A}\mathbf{y} - \mathbf{b}^T\mathbf{y} + c, \quad -\infty \leq \mathbf{y}_{\text{low}} \leq \mathbf{y} \leq \mathbf{y}_{\text{up}} \leq +\infty. \quad (19)$$

The problem with standardly applied algorithms is that the matrix **A** might not necessarily be calculated in an explicit way. The terms which arise from the first two integrals in the right-hand side of (16) provide the energy and calculating the derivative with respect to the unknown **v** they provide a projected traction **Mt** with **M**. The projected traction can naturally be calculated from the SGBEM algorithm, represented by the product **Ay** in equation (19). Thus, each time the optimization algorithm requires a matrix-by-vector product actually a system from the SGBEM is solved. The influence matrices of the SGBEM, however, are calculated only once at the beginning of the solution process, as they are the same for all the iterations and all time steps, considering only small displacements.

3.4 NUMERICAL EXAMPLE

The present formulation of two-domain contact problem has been tested numerically by a computer code, which was implemented in MATLAB. The developed numerical algorithm exploits the variationally based Symmetric Galerkin Boundary Element Method to calculate the elastic solution at the interface and in each subdomain. An example analysis presents the response of the cohesive contact model with friction in combination with small amount of viscosity. The geometry in the present example includes two rectangular domains mutually joined and put on each other. The bottom domain is fixed along its bottom side to a rigid foundation. The applied loading is assumed on the top domain in two subsequent steps, see Figure 3. First, a vertical compress loading is applied which leads after the rupture of the interface to a receding contact problem. Second, a loading equivalent to standard pull-push shear test well known from several engineering applications is applied afterwards. The loading process defines the prescribed displacements (*hard-device loading*) are increasing during the first phase of the loading process. The incrementally prescribed loading is given by the relation $w_2^k{=}v\tau^k$, $k{=}1,2,\ldots 100$ with $v{=}1\text{mm}\,\text{s}^{-1}$ and $\tau^k{=}k\tau_0$, $\tau_0{=}2{\times}10^{-5}$s. The first-increment of the horizontal displacement w starts for $w_1^{151} = 2\times10^{-5}$mm and it is further multiplied by a *load step factor* $(k-150)$, changing from the initial value $k{=}151$ until the total damage of the interface becomes. In total was considered $k{=}420$ load steps during the whole loading process. The geometry of the plane strain model and load configuration are conspicuous from Figure 3.

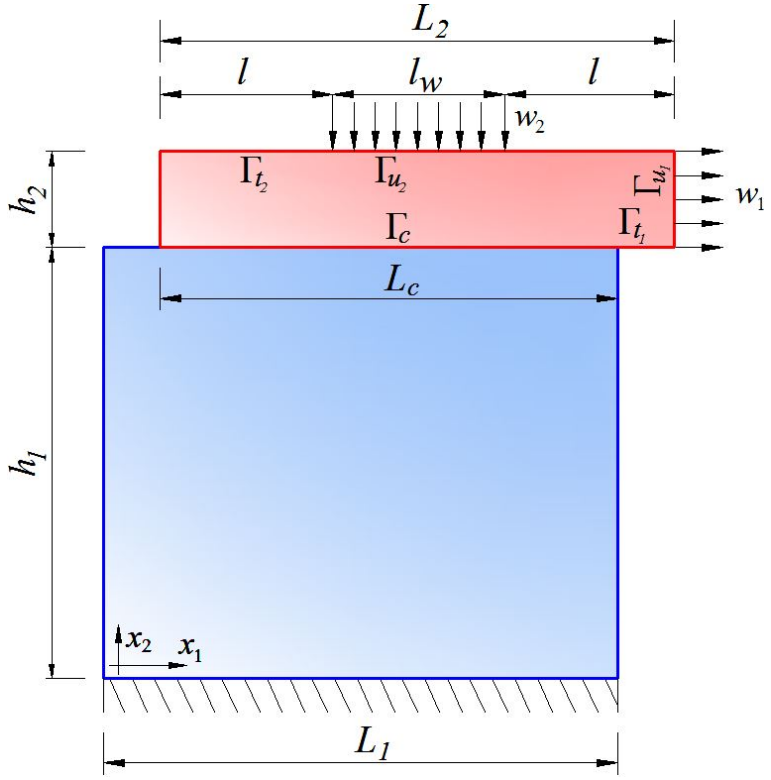

Figure 3: Geometry of the two domain example.

3.5 Model properties and parameter statement

The dimensions of the top layer are L_2=200mm and h_2=40mm. This bulk is made of aluminum with Young's modulus E=7×10^{4}MPa and Poisson's ratio ν=0.35. It is considered that prior to loading, this bulk layer is glued to the bottom layer along a part of its bottom side in the extent of L_c=180mm. For the first case of loading the top layer is loaded along the middle part of the top face, where the given length parameters are l=$\frac{7}{16}L_2$, l_{w}=$\frac{1}{8}L_2$, whereas for the second shear loading the bulks are joined along the whole length of interface L_c. The dimensions of the bottom bulk layer are L_1=200mm and h_1=200mm with elastic properties E=7×10^{4}MPa and ν=0.35. The assumed cohesive interface material is epoxy resin, with Young's modulus E_c=2.4×10^{3}MPa and Poisson's ratio ν_c=0.35. The corresponding stiffness parameters were suggested according to the cohesive contact model: the interface stiffness is defined by k_n and k_s: k_n=1.4815×10^{3}MPa mm^{-1}, k_s=0.7408×10^{3}MPa mm^{-1}. In order to obtain continuous non-linear response of the investigated variables, both normal and tangential stiffnesses were split into two parts according to the relations: k_n=k_{n_1}+k_{n_2}, k_s=k_{s_1}+k_{s_2}, k_{n_1}=0.01 × k_n, k_{n_2}=0.99 × k_{n_1}, k_{s_1}=0.01 × k_s, k_{s_2}=0.99 × k_{s_1}. It is necessary to emphasize that cohesive contact approach requires to consider more toughness at cohesive stiffness k_{s_2} which is related to quadratic term ζ^2 in interface stored energy functional as e.g. in (16). Thereby, the non-linear response of investigated variables and continuous response has been acquired as

well. The time-relaxation parameter for the visco-elastic model is τ_R=1×10^{-4}s. The Coulomb friction coefficient is μ=0.8. The principal parameters that govern the crack propagation are: the fracture energy in Mode I G_d=10 Jm^{-2} and the viscosity parameter α=0.001Jm^{-2}s.

3.6 Result of the analysis of the contact model

The achieved numerical solution of investigated interface contact model is presented in following figures. The main feature occurred in the graphs pertinent to the cohesive model is the continuous non-linear response of the mechanical stress t and damage parameter ζ, see Figure 4, 5. The Figure 4 presents the evolution of the normal and tangential stress at the distance $x_1 = 200$mm, for whole loading process at each loadstep k.

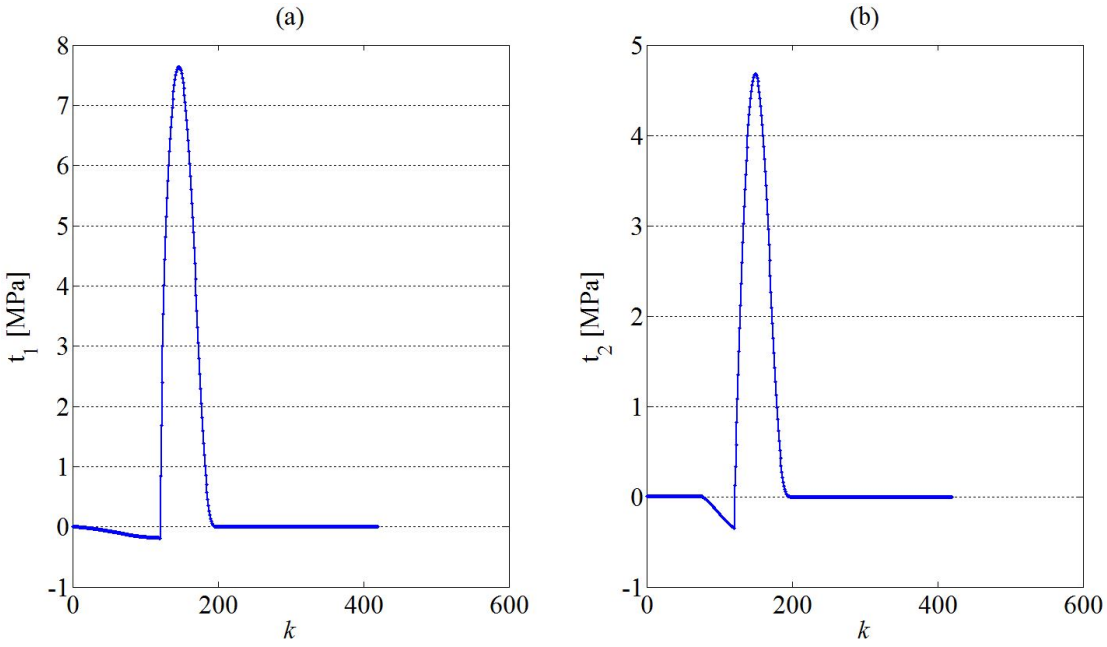

Figure 4: Distribution of (a) mechanical stress t_1, (b) mechanical stress t_2.

The influence of cohesive continuous dependence is obvious, after the system reaches the required amount of fracture energy G_d. The presented continuity of the stress also captures the influence of non-linear viscosity effect, in the stress peak of the graph. In agreement with aforementioned cohesive-contact theory [3], let us mention that the evolution of damage parameter ζ changes from one to zero continuously and thus preserves the continuous character of the debonding process, see Figure 5. Figure 6 captures the evolution of the deformation process of the layered structure. First, the structure is subjected to pressure load test w_2, which yields compressed deformation, see Figure 6(a), (b). Second, the shear load w_1 is applied on the top layer. This yields the deformation in tangential direction, such the delamination process at interface occurs, see Figure 6(c),(d).

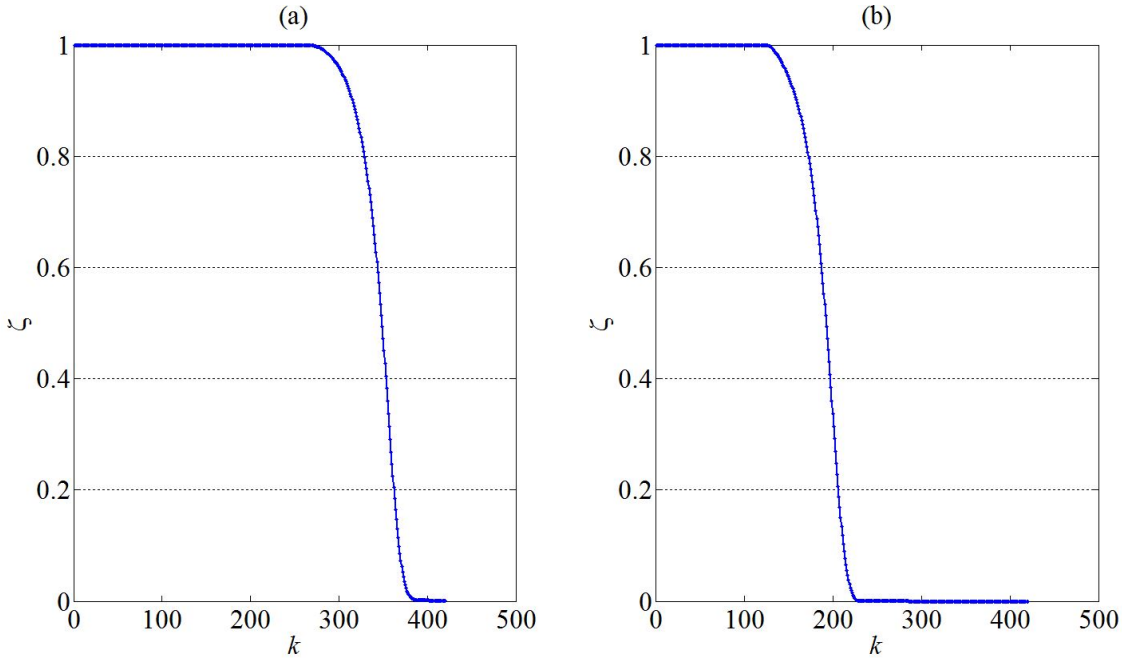

Figure 5: Distribution of damage parameter ζ at distance (a) $x_1 = 150$mm, (b) $x_1 = 200$mm.

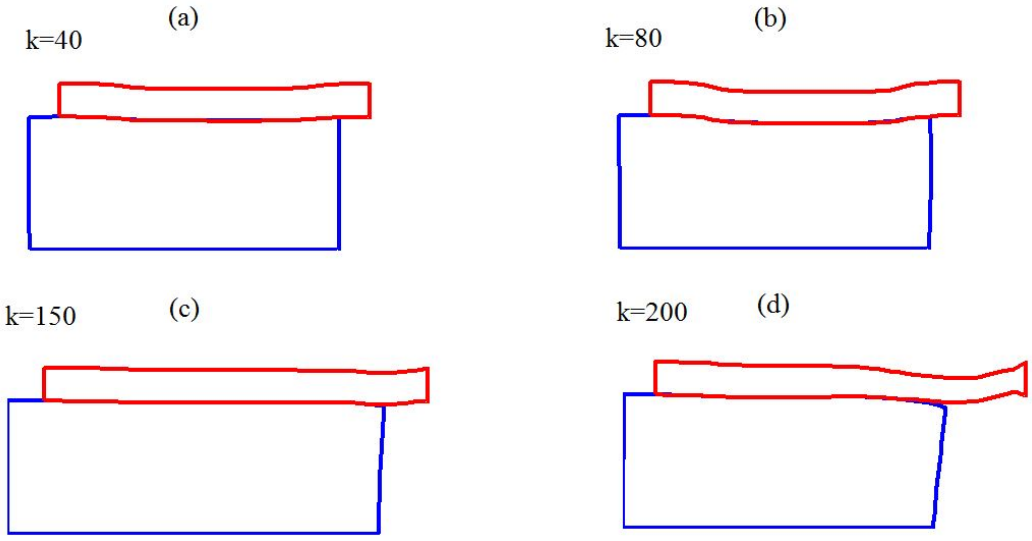

Figure 6: Evolution of multidomain deformation during the pressure load test (a,b) and shear test (c,d).

4 CONCLUSIONS

An energy based model for solving the cohesive contact with effects of viscosity and friction has been considered. The contact model provides an approach which was obtained by combining the cohesive type contact and a small amount of viscosity to make the solution more regular. The numerical implementation of spatial discretization *via* SGBEM has permitted the whole problem to be defined only by a boundary and interface data. A simple 2D contact example has been analyzed and has yielded the model response during the applied pressure and shear test, respectively. Developed cohesive approach was obtained by mere adding a new energy term with a new cohesive stiffness parameters providing required non-linear continuous dependence of the investigated parameters. The proposed numerical model confirms the expected behaviour in accordance with the applied theory and asses its applicability in several aspects of engineering practise.

5 ACKNOWLEDGEMENT

The authors are grateful for financial support of scholarship award from International Association for Computational Mechanics. The authors acknowledge the financial support from Grant Agency of Slovak Republic. The project registration number is VEGA 1/0201/11. The work was also supported by Slovak Academic Information Agency through the National Scholarship Programme of the Slovak Republic.

REFERENCES

[1] Dostál, Z. *Optimal Quadratic Programming Algorithms*, *Springer Optimization and Its Applications*, Springer, Berlin, Vol. 23, (2009).

[2] Roubíček, T., Panagiotopoulos, C.G. and Mantič, V. Quasistatic adhesive contact of viscoelastic bodies and its numerical treatment for very small viscosity. *ZAMM – Zeitschrift Angew. Math. Mech.* Vol.93, (2013).

[3] Roubíček, T., Kružík, M. and Zeman, J. *Delamination and adhesive contact models and their mathematical analysis and numerical treatment (Chapter 9)*. In V. Mantič, editor, *Mathematical Methods and Models in Composites*, Imperial College Press (2013).

[4] Vodička, R. and Mantič, V. An SGBEM implementation with quadratic programming for solving contact problems with Coulomb friction. *Advances in Boundary Element and Meshless Techniques XIV*, Eastleigh : EC ltd. (2013) 444–449.

[5] Vodička, R., Mantič, V. and París, F. Symmetric variational formulation of BIE for domain decomposition problems in elasticity - an SGBEM approach for nonconforming discretizations of curved interfaces. *CMES – Comp. Model. Eng.* (2007) 17:173–203.

[6] Vodička, R., Mantič, V. and Roubíček, T. An SGBEM implementation of quasi–static rate–independent mixed-mode delamination model. Submitted to *Meccanica* (2014).